5.1 CROSS-TROPOPAUSE TRACER TRANSPORT IN MIDLATITUDE CONVECTION

Gretchen L. Mullendore*, Dale R. Durran and James R. Holton
University of Washington, Seattle, Washington

1. INTRODUCTION

The lowermost stratosphere is defined as the section of stratosphere in the extratropics located below the 380K isentrope and above the 2 PVU potential vorticity surface (Holton et al., 1995). There are 3 pathways by which air can be transported into the lowermost stratosphere: 1) diabatic descent from the upper stratosphere, 2) isentropic transport from the lower latitude troposphere, and 3) upward diabatic transport from the midlatitude troposphere. The only pathway which could possibly transport midlatitude near surface, short-lived tracers to the lowermost stratosphere would be pathway 3, specifically deep convective transport. Even small amounts of near surface air penetrating into the lower stratosphere can have important effects on the local stratospheric chemistry, possibly affecting the entire latitude band.

Several field experiments and numerical simulations have demonstrated the important role thunderstorms play in the redistribution of trace gases in the troposphere (e.g. Wang and Chang, 1993, Hauf et al., 1995), but very few have specifically dealt with the issue of cross-tropopause exchange. In the few models that have included analysis of cross-tropopause transport due to deep convection (e.g. Stenchikov et al., 1996, Skamarock et al., 2000), the tropopause is defined by a single altitude or pressure level, but the tropopause location is unclear in the highly perturbed environment above an active storm.

Thus, to determine the irreversibility of cross-tropopause transport in simulated storms, six-hour simulations are carried out to cover the growth and decay cycles of the storm. After the decay of convection, isentropes relax to quasi-flat surfaces, allowing more confident tropopause location.

2. NUMERICAL MODEL

The model used is a three-dimensional, cloud-resolving mesoscale model following Piani et al. (2000). Scalar variables are advected using the LeVeque (1996) flux-limited scheme.

The model variables are homogeneous in the horizontal at time of initialization with the exception of boundary layer water vapor. The water vapor mixing ratio in the lowest 2 km is reduced by 50% in an area of the domain away from the initial convection. At 1.5 hours the storm propagates into the drier air which reduces environmental convective available potential energy (CAPE) and terminates the convection on a realistic timescale.

2.1 *Storm classification and initialization*

We report simulations for two storms, one supercell and one multicell. We initialized the model using idealized soundings based on the work of Weisman and Klemp (1982). The CAPE in both the multicell case and supercell case is identical (2500 m^2/s^2), but the magnitude of the low level vertical wind shear is doubled for the supercell case. There is no vertical wind shear above 5 km. Bulk Richardson number (BRN), the ratio of convective available potential energy (CAPE) to low level shear, has been used as a method of storm classification (Weisman and Klemp, 1982). The multicell has a BRN of 115, and the supercell has a BRN of 36.

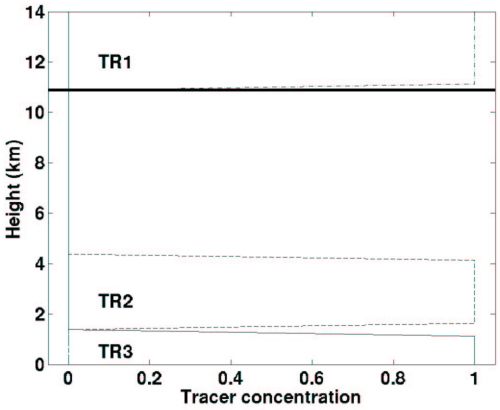

Figure 1: Vertical profiles of tracer concentrations at t=0. Heavy solid line shows tropopause location in unperturbed pre-storm environment.

2.2 *Passive tracer profiles*

To clarify the source region of air transported by the convective cloud, five passive tracers are initialized at different heights. The three most interesting tracers are show in Figure 1. For ease of discussion we shall label the tracer layers as TR3 (boundary layer) to TR1 (tropopause level to model lid). Although these tracers are idealized, they approximate atmospheric gases with specific source regions. TR3 and TR2 represent tracers with near surface sources (e.g. CO) and TR1 represents tracers with stratospheric sources (e.g. O_3). To focus on the role of transport, no chemistry was included in these runs.

**Corresponding author address:*
Gretchen L. Mullendore, Univ. of Washington, Dept. of Atmospheric Sciences, Box 351640, Seattle, WA 98195; e-mail: gretchen@atmos.washington.edu.

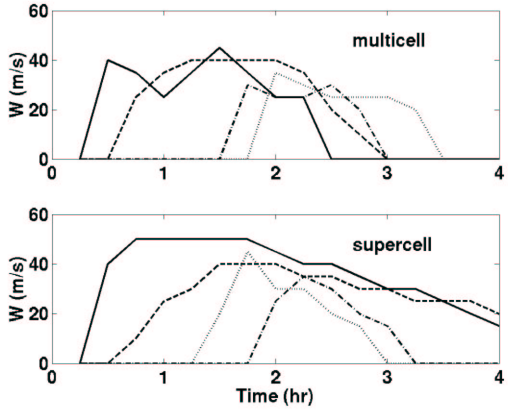

Figure 2: Vertical velocity at 7 km in the multicell (top panel) and supercell (bottom panel). Each line represents a separate cell in the model domain. Note that both regimes become more multicellular after the influx of dry air, at ~1.5 hours.

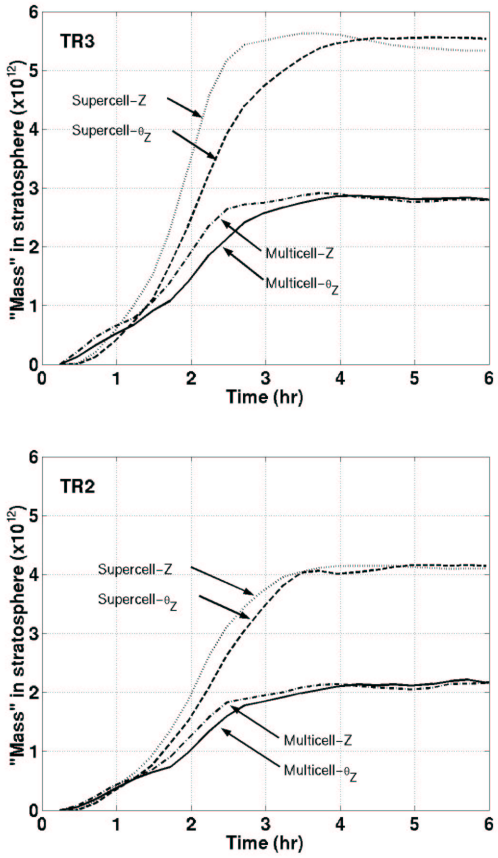

Figure 3: The total amount of TR3 (top panel) and TR2 (bottom panel) injected into the stratosphere. Supercell-Z indicates the amount injected by the supercell storm when the tropopause is defined as a single height level. Supercell-θ_Z indicates the amount injected when the tropopause is defined as a surface with an equal gradient in θ.

3. MODEL RESULTS

The supercell storm produced higher vertical velocities than the multicell storm (Figure 2). The supercell storm also maintained these high velocities for a longer time span. Due to these disparities, the supercell transported much more boundary layer air into the upper troposphere and lower stratosphere.

Figure 3 shows the total amount of TR3 (top panel) and TR2 (bottom panel) injected into the stratosphere. Although the depth of the TR3 layer is only 40% the depth of the TR2 layer, more TR3 is injected into the stratosphere. We calculated these totals using two different definitions for the tropopause. The line labeled "Supercell-Z" shows the amount injected above a single height level in the supercell storm; "Supercell-θ_Z" shows the amount injected above a surface of constant θ_Z. Total transport is similarly calculated for the multicell storm. At 6 hours into the simulation run, both tropopause definitions give similar results for the total transport. Use of the height-based tropopause definition, however, yields more mass transport into the stratosphere early in the storm's lifetime.

The y-axis of figure 3 represents the total mass of a hypothetical tracer with an initial concentration of 1 unit/m^3. CO has a typical boundary layer concentration of 1.57e-4 g/m^3 (135 ppbv). Multiplying this concentration by the total TR3 transported at 6 hours in the supercell regime, 5.54e12, gives 8.72e-4 Tg, the total mass of CO that would be transported from the lowest 1 km by the simulated storm.

Figure 4 (top panel) shows a vertical cross-section through one of the main updrafts of the supercell at 2 hours into the simulation. Figure 4 (bottom panel) shows a cross-section through that same plume at 6 hours into the simulation, after convection has become inactive and the tracer plume has been advected downstream. The thick black line depicts the location of an isosurface of θ_Z, the tropopause indicator used in this study. The tropopause location above the active updraft is unclear, but is more easily defined downwind in the less strongly perturbed environment.

In the post-storm environment, tracer plumes extend as high as 1.6 km above the tropopause. At 1 km above the tropopause, the concentration of TR3 at 6 hours into the supercell simulation has a maximum of 31% of its original concentration; the concentration of TR2 has maximum of 27% of its original concentration.

In addition to greater updraft strength and longer updraft lifetime, the greater transport in the supercell may also be due to less entrainment into the updraft core (Hauf et al., 1995). Further analysis is required to separate the various effects.

4. DISCUSSION

The above model results use static stability as an indicator of tropopause location. Most important to the study of cross-tropopause transport, however, is not transport across a surface of a given value, but the mixing of boundary layer tracers, especially short-lived tracers

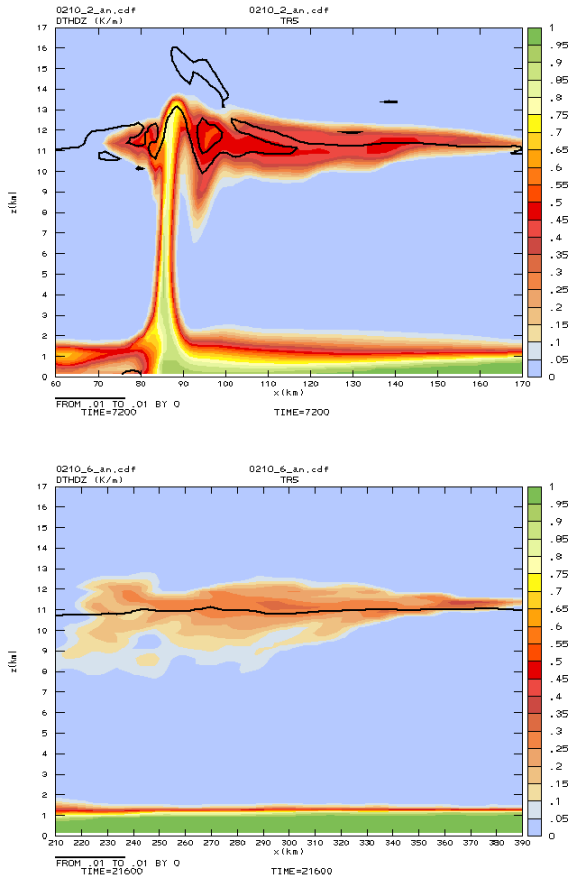

Figure 4: Vertical cross section through supercell anvil at 2 hours (top panel) and 6 hours (bottom panel). The colored contour shows the concentration of tracer TR3. The thick black line shows the location of the θ_z = 0.1 isosurface.

and/or "rare" tracers with a local source, with stratospheric tracers. There is a strong gradient in ozone at the tropopause, so ozone concentration is the best indicator of this “chemical stratosphere”. For these model runs, mixing with ozone is approximated by mixing with TR1. At 6 hours into the supercell simulation, 2200 units of TR3 have mixed with stratospheric parcels with 0.5 units or more of TR1. Additional mixing with stratospheric tracers would occur due to processes such as synoptic scale wave-breaking, a process not included in this model. A preliminary estimate gives approximately 3 days as a mixing time for the tracer plume injected above the tropopause.

Taking injection above the stability gradient as our indicator of cross-tropopause transport, the level of neutral buoyancy becomes a key component in determining the magnitude of cross-tropopause transport. Increasing the altitude of the level of neutral buoyancy in model soundings is found to produce more transport into the stratosphere. We are currently working on developing a climatological view of neutral buoyancy levels for summertime deep convection.

REFERENCES

Hauf, T., and Coauthors, 1995: Rapid vertical transport by an isolated midlatitude thunderstorm. *J. Geophys. Res.*, **100**, 22957-22970.

Holton, J.R., and Coauthors, 1995: Stratospheric-tropospheric exchange. *Rev. Geophys.*, **33**, 403-439.

LeVeque, R.J., 1996: High-resolution conservative algorithms for advection in incompressible flow. *SIAM J. Numer. Anal.*, **33**, 627-665.

Piani, C., D. Durran, and M.J. Alexander, 2000: A numerical study of three-dimensional gravity waves triggered by deep tropical convection and their role in the dynamics of the QBO. *J. Atmos. Sci.*, **57**, 3689-3702.

Skamarock, W.C., and Coauthors, 2000: Numerical simulations of the July 10 Stratospheric-Tropospheric Experiment: Radiation, Aerosols, and Ozone/Deep Convection Experiment convective system: Kinematics and transport. *J. Geophys. Res.*, **105**, 19973-19990.

Stenchikov, G. and Coauthors, 1996: Stratosphere-troposphere exchange in a midlatitude mesoscale convective complex. 2. Numerical simulations. *J. Geophys. Res.*, **101**, 6837-6851.

Wang, C. and J. Chang, 1993: A three-dimensional numerical model of cloud dynamics, microphysics, and chemistry. 3: Redistribution of pollutants. *J. Geophys. Res.*, **98**, 16787-16798.

Weisman, M.L., and J. Klemp, 1982: The dependence of numerically simulated convective storms on vertical wind shear and buoyancy. *Mon. Weather Rev.*, **110**, 504-520.